Indium-doped ZnO nanowires: Optical properties and room-temperature ferromagnetism

K. W. Liu,[a] M. Sakurai,[a] and M. Aono
International Center for Materials Nanoarchitectonics (MANA), National Institute for Materials Science (NIMS), Tsukuba 305-0044, Japan

(Received 29 April 2010; accepted 16 June 2010; published online 23 August 2010)

We report the optical and magnetic properties of ZnO, $Zn_{0.97}In_{0.03}O$, and $Zn_{0.94}In_{0.06}O$ nanowires (NWs). All samples have similar wirelike shape with an average diameter of about 70 nm and a length of about 10 μm. The comparison of photoluminescence (PL) spectra at 10 K indicated that a new broad emission band appeared after indium doping, which is associated with donor-acceptor-pair recombination. Additionally, the intensity of oxygen-vacancies-induced visible emission increased with increasing In content, indicating that In doping can induce many oxygen vacancies. Furthermore, magnetic measurements revealed that pure ZnO NWs are diamagnetic, while indium-doped ZnO NWs exhibit intrinsic ferromagnetism at room temperature. With the increase in In content, the coercive field and the magnetic moment for indium-doped ZnO NWs increase largely. Ferromagnetic ordering can be interpreted as being due to O vacancies induced by In doping, which is in good agreement with PL results. © *2010 American Institute of Physics*. [doi:10.1063/1.3464229]

I. INTRODUCTION

Quasi-one-dimensional ZnO nanostructures such as nanowires (NWs), nanobelts (NBs), and nanorods (NRs) have received tremendous attention because of their great potential applications in nanoscale electronic and optoelectronic devices.[1,2] As is well known, doping with selective elements in ZnO can realize desirable electrical, optical, and magnetic properties, which is crucial for their practical application. In particular, indium-doped ZnO (IZO) nanostructures are regarded as a promising candidate for transparent conductors,[3] gas sensors,[4] and photodetectors[5] due to their good physical properties. More recently, weak localization and electron–electron interactions have been observed in IZO NWs.[6] Furthermore, compared with ZnO doped with transition metals (Cu, Co, etc.),[7,8] IZO possesses unique figures of merit such as better optical properties and lower resistivity.[3] Hence, it is expected that IZO should be one of the most promising candidates for future spintronic devices applications. To fabricate and optimize IZO-based optoelectronic and spintronic devices, investigation of the optical and magnetic properties of IZO is of fundamental and practical importance. In previous reports, both a blueshift and a redshift in the UV emission peak were observed for IZO nanostructures fabricated by different methods.[9,10] Two residual donor levels located at about 37 and 120 meV below the conduction band minimum have been identified from the photoluminescence (PL) excitation spectra of IZO NRs.[11] Zhou *et al.*[12] found that the near-band-edge emission (NBE) of ordered IZO NWs was dominated by In-related neutral donor-bound exciton emission in low-temperature PL spectra. Although considerable effort has been devoted to the optical properties of IZO nanostructures, the detailed mechanisms underlying these properties are still not very clear. Additionally, to our knowledge, no information can be found about the magnetic properties of IZO nanostructures. In this work, ZnO and IZO NWs with different In contents were prepared on *c*-face sapphire substrates by a simple thermal evaporation technique. The effects of In doping on the optical and magnetic properties were investigated by low-temperature PL spectra and by using a superconducting quantum interference device (SQUID). Low-temperature PL spectra indicated that strong donor-acceptor-pair (DAP) emission appeared after In doping and the peak position of the excitons bound to neutral donors (D^0X) emission almost did not change. Furthermore, room-temperature ferromagnetism (RTFM) in IZO NWs was first observed in our experiment but the undoped ZnO NWs exhibited typical diamagnetic properties at 300 K.

II. EXPERIMENTAL DETAILS

The ZnO and IZO NWs with different In contents used in this study were grown on *c*-face sapphire substrates by a vapor phase transport process. Gold films with the nominal thickness of 3 nm were deposited on the substrates before the growth of ZnO NWs using as catalyst. A mixture of highly pure (99.999%) ZnO powder and (99.999%) graphite powder with a weight ratio of 1:1 ZnO/C was used as the source to prepare undoped ZnO NWs. For the growth of IZO NWs, the source was a mixture of highly pure (99.999%) ZnO powder, (99.99%) In_2O_3 powder and (99.999%) graphite powder with different weight ratios. The growth was performed at 935 °C for 40 min at a pressure of 1.3×10^3 Pa and highly pure argon mixed with 1% oxygen was used as the carrying gas. After growth, the system was cooled to room temperature. The average atomic concentration of indium in IZO NWs was estimated using energy dispersive x-ray (EDX) analysis. The morphology of the NWs was characterized by scanning

[a]Electronic addresses: sakurai.makoto@nims.go.jp and liukewei2007@yahoo.com.cn.

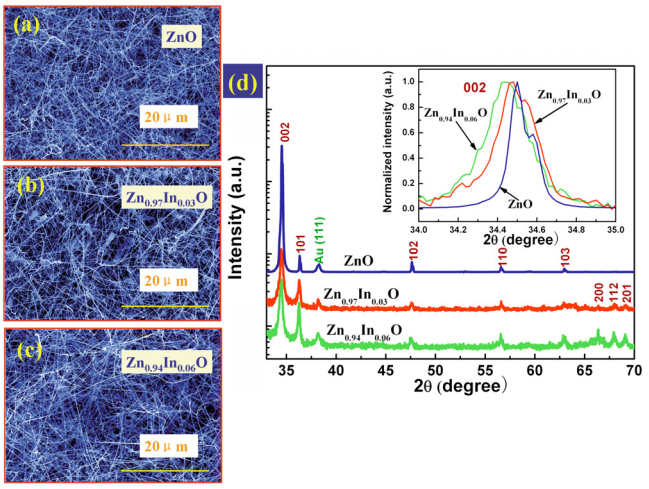

FIG. 1. (Color online) SEM images of ZnO (a), $Zn_{0.97}In_{0.03}O$ (b), and $Zn_{0.94}In_{0.06}O$ (c) NWs; (d) XRD patterns of ZnO, $Zn_{0.97}In_{0.03}O$, and $Zn_{0.94}In_{0.06}O$ NWs.

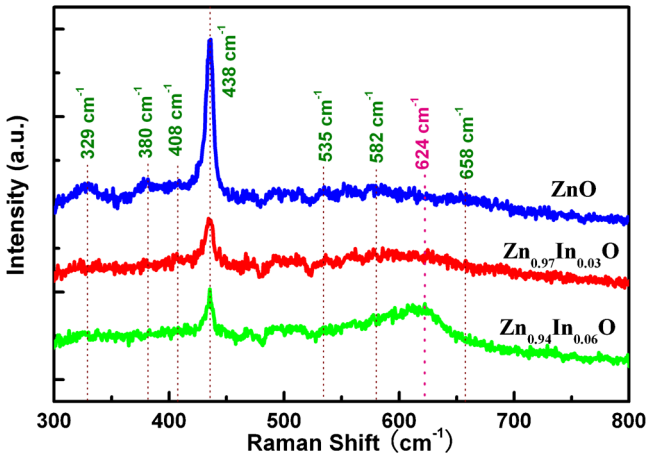

FIG. 2. (Color online) The Raman spectra of ZnO, $Zn_{0.97}In_{0.03}O$, and $Zn_{0.94}In_{0.06}O$ NWs.

electron microscopy (SEM). To investigate the local vibration modes, Raman spectra were obtained by confocal laser micro-Raman spectrometry at room temperature. The structural quality of the samples was investigated by x-ray diffraction (XRD). The PL measurements were carried out in a liquid He cryostat between 10 and 300 K using a He–Cd laser (325 nm line). Magnetic measurements were performed using a SQUID magnetometer with the magnetic field perpendicular to the substrate surface.

III. RESULTS AND DISCUSSION

Figures 1(a)–1(c) show the SEM images of ZnO, $Zn_{0.97}In_{0.03}O$, and $Zn_{0.94}In_{0.06}O$ NWs, respectively. It can be seen that three samples have similar wirelike shape with an average diameter of about 70 nm and a length of about 10 μm. The NWs are disordered in all samples. Meanwhile, it should be noted that there are few NBs dispersing in NWs in three samples (less than 2% in quantity). The SEM results indicated that three samples have the similar morphology and density. Furthermore, the samples in our case have the same size and thickness, so we can compare the optical and magnetic properties purely induced by In doping. The XRD patterns of three samples were shown in Fig. 1(d). Pure ZnO NWs can be indexed as the wurtzite hexagonal structure. After In doping, the intensity of major diffraction peak decreased, indicating that the indium doping can lead to the degradation of crystallinity. Meanwhile, Au (111) peak can be also observed for all samples. It can be noted that no obvious diffraction peaks of In_2O_3 can be found in our samples. With increasing In content, (002) peak shifts to lower angle side and becomes broader [see the inset of Fig. 1(d)]. This peak shift may be due to that the ionic radius of In^{3+} (0.071 nm) is larger than that of Zn^{2+} (0.060 nm). Peak broadening in the inset of Fig. 1(d) is caused by the degradation of crystallinity. The XRD result clearly suggests the incorporation of In into ZnO lattice without altering the crystal structure.

In order to disclose the influence of In doping on the vibrational property of ZnO NWs, the Raman scattering measurement was carried out at room temperature. Figure 2 shows the Raman spectra of ZnO, $Zn_{0.97}In_{0.03}O$ and $Zn_{0.94}In_{0.06}O$ NWs. The Raman spectrum from the undoped ZnO NWs is in good agreement with that of wurtzite ZnO.[13] The peaks at 329 cm^{-1}, 380 cm^{-1}, 408 cm^{-1}, 438 cm^{-1}, 535 cm^{-1}, 582 cm^{-1}, and 658 cm^{-1} are related to the $E_2^{high}-E_2^{low}$, $A_1(TO)$, $E_1(TO)$, E_2^{high}, $2B_1^{low}$ (2LA), $A_1(LO)$, and TA+LO, respectively.[13] After In doping, all these peaks became weaker and no significant shift in the peak position could be observed. The decrease in the intensity of E_2^{high} mode indicated that the indium ions doped into the ZnO lattice substituting for Zn.[9,14] In Fig. 2, it should be noted that an additional vibration modes appear at 624 cm^{-1} in the Raman spectrum after In doping. Furthermore, with increasing the indium content in IZO NWs, this new peak becomes stronger while other peaks become weaker. According to previous reports, this new peak should be related to indium impurities.[14–16]

Figure 3(a) shows the PL spectra of ZnO, $Zn_{0.97}In_{0.03}O$, and $Zn_{0.94}In_{0.06}O$ NWs at $T=10$ K. As can be seen, the visible emission (VE) due to the deep level defect emission from undoped ZnO NWs is very weak and almost unnoticeable at 10 K. After In doping, the intensity ratio of NBE/VE decreases. And for $Zn_{0.94}In_{0.06}O$ NWs, the intensity of NBE is stronger than that of VE. According to previous report,[17] the deep level defect emission is usually attributed to oxygen vacancies. The increase in VE intensity after In doping indicated that In doping can induce many oxygen vacancies. Interestingly, on the high-energy side of the VE band for all samples, we observed a series of small peaks with vibration characteristics related to the strong electron-longitudinal optical (LO) phonon coupling.[17] In these vibration peaks, the energy separation between any two adjacent fine peaks was found to be 66–71 meV corresponding to the LO phonon energy (72 meV) for ZnO. Figure 3(b) shows the NBE bands for three samples at 10 K. For undoped ZnO NWs, the PL spectrum is dominated by the bound-exciton emission peak at 3.358 eV, which likely originates from D^0X according to our previous work.[18] The small peak at the high-energy side of D^0X should be attributed to surface bound excitons (SX) because its thermal quenching rate is much faster than that of

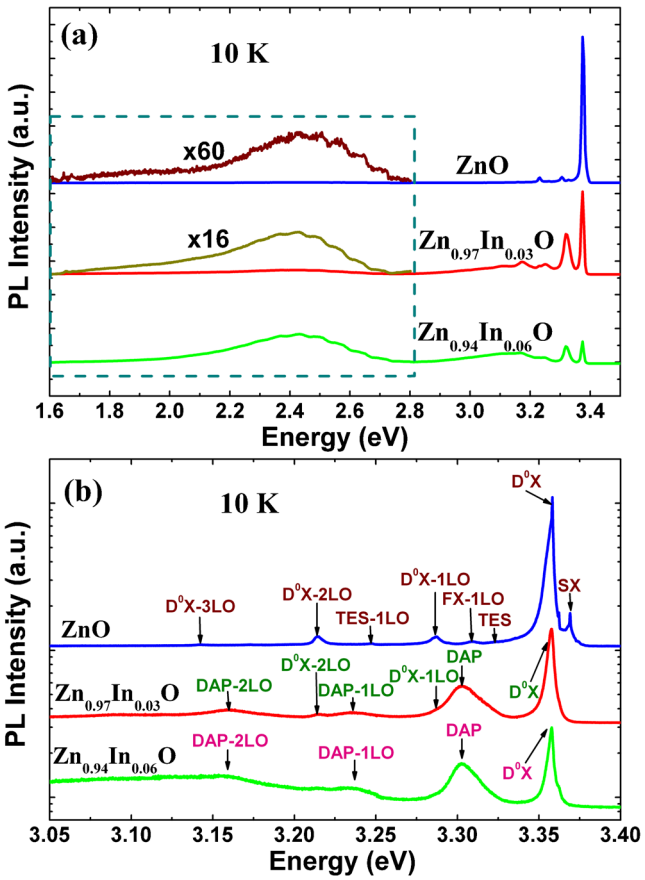

FIG. 3. (Color online) PL overview spectra (a) and NBE bands (b) of ZnO, $Zn_{0.97}In_{0.03}O$, and $Zn_{0.94}In_{0.06}O$ NWs at $T=10$ K.

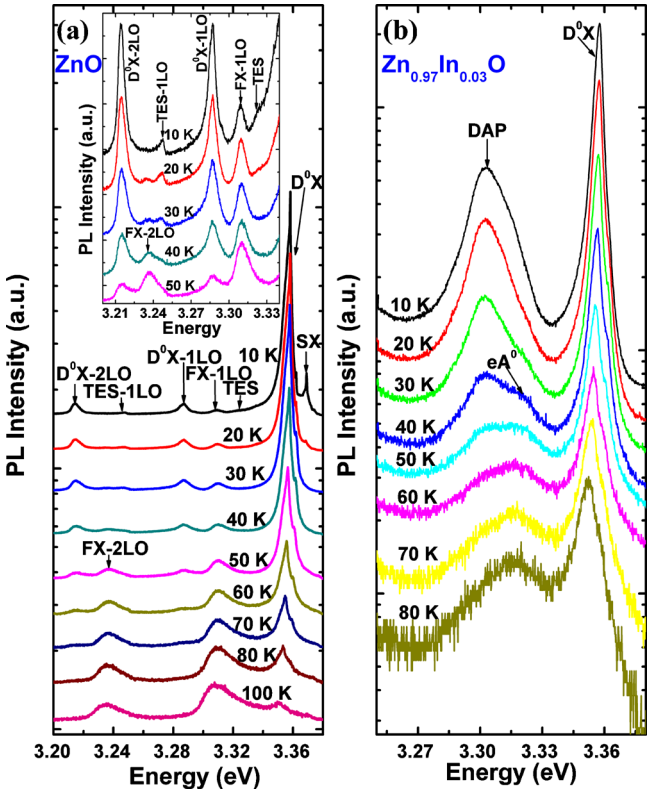

FIG. 4. (Color online) Temperature-dependent PL spectra of ZnO (a) and $Zn_{0.97}In_{0.03}O$ (b) NWs.

D^0X and it completely disappeared at 30 K (shown latter).[19] On the low-energy side of D^0X, the peak with low intensity at 3.322 eV should come from two-electron satellite (TES) of D^0X.[20] In such a transition process, the radiative recombination of a D^0X complex transfers its donor electron from the 1s ground state into an excited state such as 2*s*, 2*p*, etc.[21] Notably, the peak at 3.309 eV is associated with LO phonon replica of free exciton (FX), although we did not observe the FX emission. According to the LO phonon energy of ZnO (72 meV), the peaks at 3.286 eV, 3.247 eV, 3.214 eV, and 3.143 eV can be attributed to D^0X-1LO, TES-1LO, D^0X-2LO, and D^0X-3LO, respectively. After doping with indium, the PL spectra exhibit many different features compared to that of pure ZnO NWs. The SX emission disappears completely for IZO NWs. The intensity of D^0X decreases but the peak position is almost no change, which is different from Ref. 12. According to previous reports, In-related D^0X usually occurs at 3.357 eV.[12,22] In this experiment, D^0X of undoped ZnO NWs appears at 3.358 eV, so it is difficult to identify the emission associated with In donor bound exciton after In doping. At 3.303 eV, a new broad emission band can be clearly observed, which is attributed to DAP recombination.[20] The FX-1LO may have merged into this emission band and cannot be identified clearly in these spectra. Additionally, the intensity of DAP recombination band increases with the increase in In content, indicating that this emission is related to indium doping.

In order to further investigate the effect of In doping on optical properties of ZnO, the temperature-dependent PL spectra measurements were carried out by using a liquid He cryostat. Figures 4(a) and 4(b) show the temperature-dependent PL spectra of ZnO and $Zn_{0.97}In_{0.03}O$, respectively. As can be seen in Fig. 4(a), the intensity of D^0X decreases readily and the peak shifts toward lower energy with the increase in temperature. Since D^0X partially thermally dissociates into FX, the attenuation of FX-LO phonon replicas with increasing temperature is much slower in comparison with D^0X. Consequently, when the temperature is higher than 100 K (not shown), FX-1LO and FX-2LO become the dominant emissions and the peak intensities are higher than that of the D^0X peak. A similar behavior is observed from the NBE band of ZnO tetrapods.[23] Meanwhile, the SX emission disappeared completely at 30 K. The inset of Fig. 4(a) shows a magnified image of the spectra in the range from 3.2 to 3.34 eV. It can be clearly seen that the TES and TES-1LO peaks decrease rapidly in intensity with increasing temperature and vanish when the lattice temperature exceeds 40 K. The disappearance rate of the TES band is much faster than that of D^0X band. This corresponds to the fact that the TES band cannot exist without its primitive D^0X emission.[24] After doping with indium, the DAP emission band appeared and the SX emission disappeared. Taking a close look at the DAP emission band shown in Fig. 4(b), it can be seen that this line is much broader than the D^0X line. The identification of DAP transition is further confirmed by a new peak at the high energy side of the DAP emission corresponding to free-electron-to-acceptor (eA^0) at higher temperature. It was found that the energy distance between DAP and eA^0 is

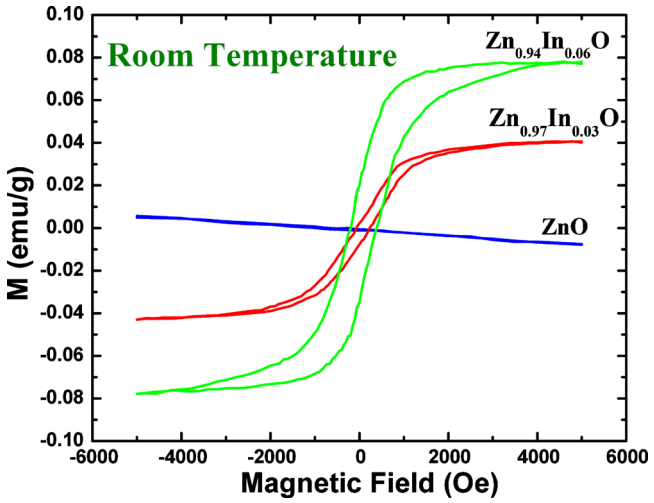

FIG. 5. (Color online) Magnetization curves of ZnO, $Zn_{0.97}In_{0.03}O$, and $Zn_{0.94}In_{0.06}O$ NWs at room temperature.

around 15 meV. This value is similar to that in previous reports.[20] As is well known, the eA^0 transition energy (E_{eA}) can be expressed as the following equation:[25]

$$E_{eA} = E_g - E_A + k_B T/2, \quad (1)$$

where E_g is the band-gap energy, E_A is the binding energy of the acceptor, T is the temperature, and k_B is the Boltzmann constant. The band-gap energy can be estimated by the PL peak of FX-1LO from undoped ZnO NWs ($E_{\text{FX-1LO}}$), the LO phonon energy (72 meV), and the binding energy (60 meV) of FX. At 40 K, $E_{\text{FX-1LO}}=3.308$ eV and $E_{eA}=3.320$ eV, the acceptor binding energy was estimated to be around 122 meV, which is in good agreement with the value in Ref. 26 (130 ± 3 meV). The stacking faults may act as acceptors and the introduction of indium into ZnO is expected to lower the threshold for stacking faults formation.[26] Additionally, dangling bonds which can form localized electronic states can also be responsible for the acceptorlike defect states.[26]

Magnetization measurements carried out at room temperature for three samples are shown in Fig. 5. The substrate effect has been subtracted. In this figure, the curves corresponding to the IZO NWs show a characteristic hysteresis loop, confirming the ferromagnetic nature of these NWs at room temperature. The undoped ZnO NWs exhibit purely diamagnetic behavior at 300 K. With the increase in In content, the coercive field and the magnetic moment for IZO NWs increase largely. Many mechanisms can be responsible for this RTFM. Au catalysts may have contributed to this RTFM. However, three samples are prepared and measured at the same conditions, so the effect of Au catalysts should be similar for all samples. Additionally, the undoped ZnO NWs do not exhibit RTFM at 300 K. So the effect of Au catalysts can be ruled out. Considering that the undoped ZnO NWs exhibit purely diamagnetic and the magnetic moment increases with increasing In content, we conclude that RTFM in IZO NWs should be caused by indium doping. EDX, XRD, and Raman results indicate that there are no other magnetic elements or obvious separate phase in IZO NWs. Additionally, indium and indium-related oxides are nonferromagnetic.[27] Hence, the origin of ferromagnetism cannot be the impurity phase in the IZO NWs. According to previous reports, the defects such as O or Zn vacancies in ZnO can realize RTFM.[28,29] Therefore, the RTFM in IZO may be associated with O vacancies caused by In doping. This result is in good accordance with the strong VE after doping with indium in PL spectra.

IV. CONCLUSION

In summary, ZnO and IZO NWs have been prepared and investigated. XRD and Raman results showed that indium ions doped into the ZnO lattice without the presence of any second phase. Low-temperature PL spectra indicated that NBE band of undoped ZnO was dominated by D^0X with some weak peaks (SX, TES, FX-LO, and D^0X-LO). After In doping, a new broad emission band appeared, which is associated with DAP recombination. The binding energy of the acceptor was estimated to be about 122 meV from temperature-dependent PL spectra. Additionally, the RTFM was clearly observed in IZO NWs, which may be associated with O vacancies induced by In doping. The coercive field and the magnetic moment for IZO NWs increase with the increase in In content. Our work suggests that doping ZnO with indium is a viable approach to realizing high-quality optical properties and RTFM, which may help to advance optoelectronic and spintronic devices.

ACKNOWLEDGMENTS

The authors would like to express their gratitude to Dr. Y. Wada for preparing the low-temperature PL experiments. This work was supported in part by the World Premier International Research Center (WPI) Initiative on Materials Nanoarchitectronics, MEXT, Japan.

[1] C. Soci, A. Zhang, B. Xiang, S. A. Dayeh, D. P. R. Aplin, J. Park, X. Y. Bao, Y. H. Lo, and D. Wang, Nano Lett. **7**, 1003 (2007).
[2] Y. Xia, P. Yang, Y. Sun, Y. Wu, B. Mayer, B. Gates, Y. Yin, F. Kim, and H. Yan, Adv. Mater. **15**, 353 (2003).
[3] T. Minami, H. Sonohara, T. Kakumu, and S. Takata, Jpn. J. Appl. Phys., Part 2 **34**, L971 (1995).
[4] B. L. Zhu, D. W. Zeng, J. Wu, W. L. Song, and C. S. Xie, J. Mater. Sci.: Mater. Electron. **14**, 521 (2003).
[5] P.-T. Liu, Y.-T. Chou, and L.-F. Teng, Appl. Phys. Lett. **94**, 242101 (2009).
[6] R. S. Thompson, D. Li, C. M. Witte, and J. G. Lu, Nano Lett. **9**, 3991 (2009).
[7] D. Chakraborti, J. Prater, and J. Narayan, Appl. Phys. Lett. **90**, 062504 (2007).
[8] Z. W. Zhao, B. K. Tay, J. S. Chen, J. F. Hu, B. C. Lim, and G. P. Li, Appl. Phys. Lett. **90**, 152502 (2007).
[9] Y. W. Chen, Y. C. Liu, S. X. Lu, C. S. Xu, C. L. Shao, C. Wang, J. Y. Zhang, Y. M. Lu, D. Z. Shen, and X. W. Fan, J. Chem. Phys. **123**, 134701 (2005).
[10] J. Jie, G. Wang, X. Han, Q. Yu, Y. Liao, G. Li, and J. G. Hou, Chem. Phys. Lett. **387**, 466 (2004).
[11] H. P. He, Z. Z. Ye, S. S. Lin, H. P. Tang, Y. Z. Zhang, L. P. Zhu, J. Y. Huang, and B. H. Zhao, J. Appl. Phys. **102**, 013511 (2007).
[12] H. Zhou, J. Fallert, J. Sartor, R. J. B. Dietz, C. Klingshirn, H. Kalt, D. Weissenberger, D. Gerthsen, H. Zeng, and W. Cai, Appl. Phys. Lett. **92**, 132112 (2008).
[13] R. Cuscó, E. Alarcón-Lladó, J. Ibáñez, L. Artús, J. Jiménez, B. Wang, and M. J. Callahan, Phys. Rev. B **75**, 165202 (2007).
[14] K. J. Chen, F. Y. Hung, and S. J. Chang, J. Nanosci. Nanotechnol. **9**, 3325 (2009).
[15] L. W. Yang, X. L. Wu, G. S. Huang, T. Qiu, and Y. M. Yang, J. Appl. Phys. **97**, 014308 (2005).
[16] C. Bundesmann, N. Ashkenov, M. Schubert, D. Spemann, T. Butz, E. M.

Kaidashev, M. Lorenz, and M. Grundmann, Appl. Phys. Lett. **83**, 1974 (2003).
[17]J. Grabowska, A. Meaney, K. K. Nanda, J. P. Mosnier, M. O. Henry, J. R. Duclere, and E. McGlynn, Phys. Rev. B **71**, 115439 (2005).
[18]K. W. Liu, R. Chen, G. Z. Xing, T. Wu, and H. D. Sun, Appl. Phys. Lett. **96**, 023111 (2010).
[19]L. Wischmeier, T. Voss, I. Rückmann, J. Gutowski, A. C. Mofor, A. Bakin, and A. Waag, Phys. Rev. B **74**, 195333 (2006).
[20]B. P. Zhang, N. T. Binh, Y. Segawa, K. Wakatsuki, and N. Usami, Appl. Phys. Lett. **83**, 1635 (2003).
[21]K. Thonke, T. Gruber, N. Teofilov, R. Schonfelder, A. Waag, and R. Sauer, Physica B **308–310**, 945 (2001).
[22]B. K. Meyer, H. Alves, D. M. Hofmann, W. Kriegseis, D. Forster, F. Bertram, J. Christen, A. Hoffmann, M. Straßburg, M. Dworzak, U. Haboeck, and A. V. Rodina, Phys. Status Solidi B **241**, 231 (2004).
[23]Y. Zhong, A. B. Djurisic, Y. F. Hsu, K. S. Wong, G. Brauer, C. C. Ling, and W. K. Chan, J. Phys. Chem. C **112**, 16286 (2008).
[24]M. T. Htay, M. Itoh, Y. Hasimoto, and K. Ito, Jpn. J. Appl. Phys. **47**, 541 (2008).
[25]Y. R. Ryu, T. S. Lee, and H. W. White, Appl. Phys. Lett. **83**, 87 (2003).
[26]M. Schirra, R. Schneider, A. Reiser, G. M. Prinz, M. Feneberg, J. Biskupek, U. Kaiser, C. E. Krill, K. Thonke, and R. Sauer, Phys. Rev. B **77**, 125215 (2008).
[27]N. H. Hong, J. Sakai, N. T. Huong, and V. Brizé, Appl. Phys. Lett. **87**, 102505 (2005).
[28]V. Bhosle and J. Narayan, Appl. Phys. Lett. **93**, 021912 (2008).
[29]J. Lqbal, B. Wang, X. liu, D. Yu, B. He, and R. Yu, New J. Phys. **11**, 063009 (2009).